JOURNAL OF CATALYSIS 81, 418–428 (1983)

Xylene Isomer Diffusivity and Shape Selectivity in ZSM Zeolites[1]

R. LE VAN MAO,*,[2] V. RAGAINI,† G. LEOFANTI,* AND R. FOIS†

*Montedison S.p.A., Bollate Research Centre, Via S. Pietro 50, 20021 Bollate (MI), Italy, and †Istituto di Chimica Fisica, University of Sassari, Via Vienna 2, 07100 Sassari, Italy

Received December 8, 1981; revised September 29, 1982

Xylene isomer diffusivity in ZSM zeolites was determined via vapor sorption under constant pressure of the adsorbate. Taking into consideration the diffusion data and other sorptive properties, attempts were made to correlate the crystalline characteristics of the ZSM samples with their catalytic activity for *meta*-xylene isomerization. In particular, large ZSM-5 crystalline particles were found to be more selective (to *para*-xylene) but less active than the smaller isostructural particles. This enhanced shape selectivity is ascribed to a screening effect due to a silica binding deposit within the large particles.

INTRODUCTION

The great interest in the ZSM zeolites can be ascribed to their ability to perform many reactions with very good yield and to the high selectivity reached in some cases. The so-called shape selectivity in the ZSM type zeolites has found a fertile application in various catalytic processes (isomerization, alkylation, and transalkylation of alkylaromatics, gasoline production from methanol, etc.). Since structural characteristics of zeolites are frequently considered as determining factors in their catalytic activity, the present work aims to check these statements experimentally by comparing the diffusive and catalytic properties of two structurally different ZSM zeolites (ZSM-5 and ZSM-11, as claimed in the patent literature). The samples chosen for this study have a great number of very similar physicochemical characteristics.

Another objective is to determine whether within the ZSM-5 structure, properties such as size and distribution of crystalline particles, sorption behavior and capacity, diffusion, etc., are able to justify deep differences in *para*-xylene selectivity observed in the *meta*-xylene isomerization reaction. In particular, diffusion data with xylene isomers may help one to understand how the 10-membered ring of the ZSM channels can discriminate between the isomeric molecules which diffuse or counter-diffuse within the zeolite structure. As the cross-sections of these molecules are of the same order of magnitude as the ZSM pore diameters, the effects of the shape selectivity may be emphasized.

The method and apparatus are described elsewhere (*1, 2*): the method consists essentially in allowing contact between the zeolite samples and the adsorbate under constant pressure and in a closed (static) system. Xylene diffusivities are determined by means of a formula proposed by Barrer (*3*), which mainly involves the sorption time-dependence of the zeolite weight and which can be seen as a simplification of a more general expression formulated by Crank (*4*). By comparison of the diffusion data between the ZSM samples, interesting conclusions about the diffusion phenomena in ZSM zeolites can be deduced.

[1] Presented in part at the 14th National Congress of the Italian Chemical Society, held in Catania, Italy in September 1981.

[2] Present address: Concordia University, Sir George Williams Campus, Department of Chemistry, 1455 De Maisonneuve West, Montreal, Quebec H3G 1M8, Canada.

0021-9517/83 $3.00

EXPERIMENTAL

ZSM zeolites were synthesized according to the literature (*5, 6*). All the zeolites were in the H-form which was obtained by first exchanging the Na^+ ions of the as-made zeolites with the NH_4^+ ions, followed by calcination at 540°C for 10 hr.

All the samples were characterized by chemical analysis (Si/Al atom ratio), X-ray diffraction (structure and degree of crystallinity), optical microscopy (mean diameter (*2*) and size distribution of the crystalline particles), scanning electron microscopy (SEM) (morphology), and gas and vapor adsorption.

Sorptive characteristics of the zeolites were studied at first by performing nitrogen adsorption. For this purpose, a modified *t*-plot method was used, which basically consists in establishing the nitrogen sorption isotherm by plotting the sorbed volume against the thickness t of the sorbed layer (*7*). The sorbed amount V_z (cm^3/g) which is a quantity directly related to the surface area of the total (inter- and intracrystalline) zeolite microporosity, was determined by extrapolating to $t = 0$ the asymptotic line of the isotherm at the maximum allowed coverage t_m. The latter was assigned the value of 5 Å since the largest zeolite pores are 10 Å in diameter. This approach is similar to that of several other works (*8–12*). Nevertheless, it can provide a very convenient means when accessible total "surfaces" of two isostructural zeolite samples have to be compared.

On the other hand, the intracrystalline pore volume V_p of a zeolite can be determined by means of the relation $V_p = x/d_a$ where x is the sorbed quantity at the relative pressure of the adsorbate $P/P_0 \simeq 1$ and d_a is the density of the liquid adsorbate (*13*); water is usually used as adsorbate. Since it was observed in the case of the silica-rich ZSM zeolites (*1, 2*) that V_p (water) $< V_p$(*n*-hexane) under relative pressures of water = 0.8 and *n*-hexane = 0.3 to 0.8 (constant value for sorbed *n*-hexane at equilibrium), sorbed *n*-hexane volume was adopted as the intracrystalline pore volume of the ZSM zeolite. The RAI index, i.e., the relative affinity in adsorption, defined as the volumetric ratio of sorbed *n*-hexane to sorbed water in zeolite, was determined as previously described (*1, 2*).

The xylene adsorption conditions are reported in Table 1. The apparatus used in the present work derives from the former version (*1, 2*) by a modification of the adsorption chamber which is now able to receive several sampling tubes (see Fig. 1). Each of them can be separately withdrawn for weighing after adsorption for a prefixed time. These tubes, made of porous material, must permit the adsorbate vapor to contact instantaneously the zeolite particles. The adsorption data are the arithmetic

TABLE 1

Xylene Adsorption Conditions

Zeolite[a]	Adsorbate	Adsorption temperature (°C)	Vaporization temperature (°C)	Adsorbate pressure[b] (Torr)
H-ZSM-11	*para*-Xylene	40	25	8.8
	meta-Xylene	40	25	8.3
	ortho-Xylene	40	25	6.6
H-ZSM-5(I)	*para*-Xylene	40	20	6.5
H-ZSM-5(II)	*meta*-Xylene	40	20	6.2

[a] Prior to any diffusion measurement, the sample was heated under a 10^{-2} Torr vacuum at 350°C for 3 hr (1 Torr = 133.3 N m^{-2}).

[b] According to Antoine's equation: $\log P = A - B/(t^\circ + C)$.

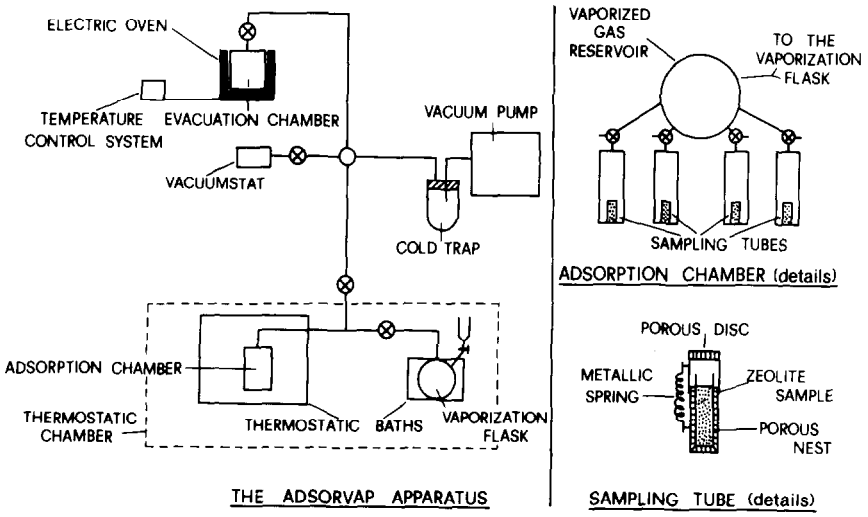

FIG. 1. The Adsorvap apparatus for vapor adsorption and diffusion studies.

means from a large number of measurements performed in the same conditions.

In order to estimate the importance of the intercrystalline adsorption in our procedure, some runs were performed with Zeolite 4A (powdered form, from Linde) which had size characteristics similar to those of the finest ZSM-5 sample. The amount of sorbed xylenes was in all cases smaller than 0.1%. Since the narrow pores of the 4A did not allow access to the bulky xylene molecules, we concluded that interparticle sorption (and thus diffusion) phenomena were negligible in our conditions of operating (see the Appendix).

The equation used for the calculation of the diffusion coefficients (*3*) concerns isothermal measurements at constant pressure of the (single) diffusant. This equation, valid for large sorption times t, is expressed as follows:

$$-\ln\frac{Q_\infty - Q_t}{Q_\infty - Q_0} = -\ln 6/\pi^2 + \frac{D}{a^2}\pi^2 t \quad (1)$$

where Q_t, Q_0, and Q_∞ are the amounts (%) sorbed at time t, when $t = 0$ and at equilibrium ($t \to \infty$), respectively, D is the diffusion coefficient, and a the particle radius. Here, we assume that $Q_0 = 0$ and that Q_∞ is the amount sorbed at $t \geq 12$ hr. For interpretative conveniency, we preferred at first to express the results as the "time-ratio" D/a^2 rather than D, to avoid the specification of the controversially defined radius a. However, attempts were made for the determination of D by assuming a to be half the mean particle diameter as measured via optical microscopy (*2*), including consequently mesopores and intracrystalline micropores of the zeolite. Therefore, the D values are representative of an overall diffusion phenomenon within the powdered zeolite pores.

Accordingly, the time-ratio will be used as the comparative factor in the discussion about the diffusion properties. When a ratio of time-ratios (referred to different adsorbates and measured on the same zeolite) is involved, the diffusion coefficients D will obviously appear in the text.

The time-ratio D/a^2 was determined from the slope of the best straight line calculated from the data of $-\ln[(Q_\infty - Q_t)/Q_\infty]$ vs t.

To show the importance of the shape selectivity occurring within the 6 Å channels of the ZSM, experimentation was made by loading the ZSM samples in a tubular reactor and then exposing the catalysts to pure *meta*-xylene vapor diluted in hydrogen (see

reaction conditions in the footnote to Table 6). The *meta*-xylene underwent isomerization to a mixture of *ortho*/*meta*/*para*-xylenes (small quantities of side-reaction products were also formed). The results are expressed in terms of thermodynamic equilibrium approach (TEQA) and C_8 aromatics (xylenes) yield (SC8): more simply, these two sets of data can be considered as the conversion and the overall selectivity, respectively. The ratios of the approaches to thermodynamic equilibrium of the main products P/O, namely *para*-xylene to *ortho*-xylene, and of *para*-xylene to *meta*-xylene, P/m, may be useful to point to an eventual diffusive "preference" of the catalyst for a particular conformation of the product molecule.

RESULTS AND DISCUSSION

Chemical Composition, Sorption Data and RAI Values

Data for three zeolite samples (one ZSM-11 and two ZSM-5, (I) and (II)) are reported in Table 2.

All the examined ZSM zeolites have nearly the same chemical composition of the H-forms. The Al/Na atom ratios of the as-made forms of the ZSM-11 and ZSM-5 (II) are nearly equal; both are different from that of the ZSM-5 (I) (Table 3).

Nitrogen sorption data (V_z) show no difference between the three zeolites; intracrystalline sorption data of *n*-hexane and of water are lower in the case of ZSM-5 (I) (Table 2), indicating probably a slight restriction in the intracrystalline accessibility of the sample involved. The RAI values of ZSM-11 and ZSM-5 (II) are very similar, while that of ZSM-5 (I) is clearly higher (Table 2); this latter fact must be mainly ascribed to a larger mean particle diameter (*2*).

Degree of Crystallinity

Since all the samples have a high degree of crystallinity as determined via X-ray diffraction (*2*), the amorphous part has not been taken into account.

Optical and Electron Microscopy

The mean diameters of the crystalline particles (Φ_m) are reported in Table 2. The ZSM-11 and ZSM-5 (II) samples have roughly the same Φ_m while that of ZSM-5 (I) is four times larger. As shown in Fig. 2, the particle size distribution of the ZSM-5 (I) is unimodal while that of ZSM-5 (II) (and also that of ZSM-11, not reported) is bimodal. The presence of cemented crystallites in the ZSM zeolites and, in particular, of some gel precursor fragments already visible in the scanning electron micrographs of the ZSM-5 (I) (Fig. 3), may indicate a zeolite formation process similar to that of a "solid hydrogel phase crystallization" as reported by Derouane *et al.* (*14*). The existence of cemented aggregates makes the de-

TABLE 2

Physical, Chemical, and Sorptive Properties of the Zeolite Samples

Zeolite	Si/Al atom ratio	Al/Na atom ratio	Φ_m[a]	Nitrogen sorption V_z[b]	Sorption capacity at 25°C[c]		
					n-Hexane	Water	RAI
H-ZSM-11	43	2.7	10.0	112	16.9	11.1	1.51
H-ZSM-5(I)	46	3.6	31.5	110	17.2	9.0	1.90
H-ZSM-5(II)	43	3.7	8.1	106	18.5	12.6	1.47

[a] Mean (volume based) particle diameter (in μm, 1 μm = 10^{-6} m) as measured via optical microscopy.
[b] Expressed in cm^3 of gas/g of dehydrated zeolite.
[c] See Ref. (*1*). The sorption capacity is expressed in cm^3 of liquid/100 g of dehydrated zeolite.

TABLE 3

Crystallization Conditions of the ZSM Samples

Zeolite samples	ZSM-5 (I)	ZSM-5 (II)	ZSM-11
Starting materials			
Aluminium	Na aluminate	Na aluminate	Na aluminate
Silicon	Ludox AS (colloidal silica)	Ludox AS	Ludox AS
Organic ion source[a]	(TPA)OH	(TPA)I	(TBA)I
Ingredients molar ratios			
Si/Al	38	41	41
Al/Na	0.92	0.12	0.13
(Si + Al)/(TPA or TBA)	2.16	9.16	17.30
(TPA or TBA)/Na	16.5	0.5	0.3
H_2O/(Si + Al)	30	26	25
Synthesis conditions			
Autoclave	Hydrothermal	Hydrothermal	Hydrothermal
Temperature (°C)	175	180	160
Time (days)	5	5	2
100% crystalline product molar ratios (as-made zeolite)			
Si/Al	43	42	42
Al/Na	3.1	1.1	1.0

[a] TPA, Tetrapropylammonium; TBA, tetrabutylammonium.

termination of the crystalline particle dimensions very difficult and should be regarded as the main cause of differences in *n*-hexane and water adsorption, and, as subsequently shown, in diffusion and catalytic selectivity.

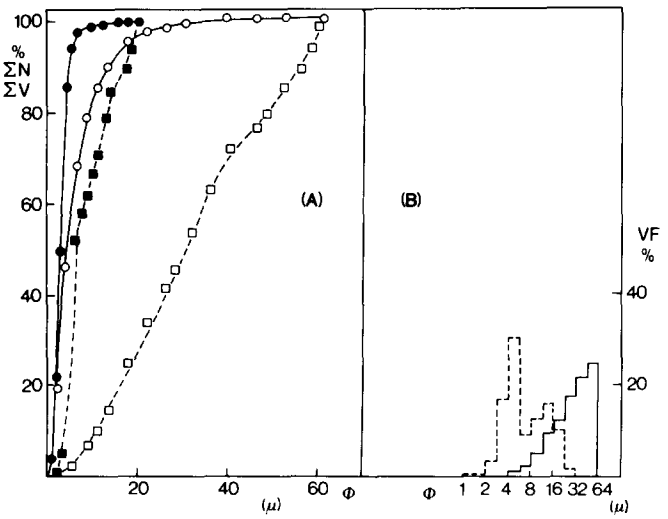

FIG. 2. (A) Numerical (ΣN) and volumetric (ΣV) percentages vs crystalline particle diameter Φ. (B) Volumetric percentage frequency distribution (VF) vs crystalline particle diameter Φ. H-ZSM-5 (II): ΣN, —●—; ΣV, --■--; VF, ---. H-ZSM-5 (I): ΣN, —○—; ΣV, --□--; VF, ——.

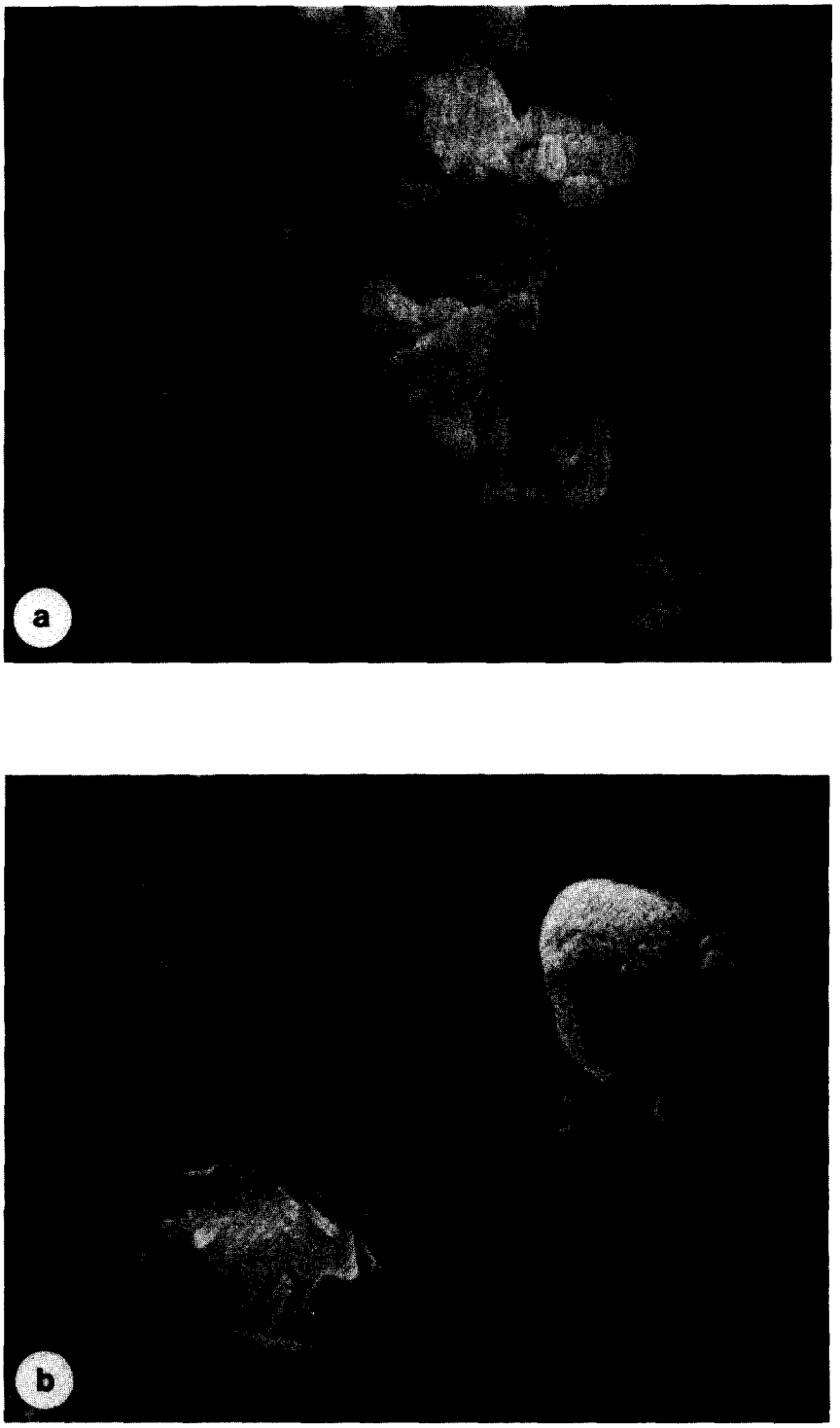

FIG. 3. Scanning electron micrographs of H-ZSM-5 (I). (a) Powdered sample, without any particular treatment (10 μm is 30 mm on the photograph). (b) sample diluted in anhydrous alcohol after vigorous shaking with ultrasound. To observe the ZSM-5 crystalline particles and the "solid gel precursor" fragments (μm is 10 mm on the photograph).

Xylene Adsorption

In Table 4 are reported the adsorption data of the xylene isomers, the calculated time-ratios (D/a^2) and the diffusion coefficients (D). In Table 5, the mean deviations (RD), the correlation coefficients (CC), and the interpolated curve intercepts A (obtained by extrapolating t to zero) are reported as reliability factors of the experimental data vs the formula used.

TABLE 4

Xylene Sorption Data

Zeolite	Adsorbate (critical diameter in Å)	Q_∞ (%)	t min	Q_t(%) Exp.	Q_t(%) Calc.	$D/a^2 \times 10^5$ (sec^{-1})	$D \times 10^{12}$ (cm^2/sec)
H-ZSM-11	*para*-Xylene	13.43	6	7.12	8.42		
	(6.7)		7	8.55	8.75	11.3	28.3
			8	9.00	9.05		
			10	10.84	9.60		
			25	11.70	12.03		
			30	12.53	12.43		
	meta-Xylene	8.08	10	3.83	3.87		
	(7.1)		15	3.92	4.49	5.34	13.4
			20	4.68	5.01		
			25	5.56	5.46		
			30	6.00	5.85		
			35	6.66	6.17		
			50	6.94	6.89		
			60	7.04	7.22		
	ortho-Xylene	9.93	10	1.72	2.15		
	(7.4)		15	2.62	3.03	4.02	10.1
			20	3.80	3.80		
			25	4.66	4.49		
			30	5.73	5.10		
			60	7.42	7.57		
H-ZSM-5	*para*-Xylene	14.21	5	6.01	7.27		
(II)	(6.7)		10	8.57	9.29	11.6	19.1
			15	11.53	10.72		
			20	12.37	11.74		
			30	12.61	12.97		
	meta-Xylene	4.75	25	2.62	2.63		
	(7.1)		30	3.13	2.99	6.44	10.6
			35	3.46	3.30		
			60	4.10	4.19		
			75	4.26	4.43		
			90	4.63	4.57		
H-ZSM-5	*para*-Xylene	11.20	5	3.71	3.00		
(I)	(6.7)		8	6.30	5.99	25.5	633
			10	6.58	7.35		
			15	9.28	9.39		
			20	10.42	10.35		
	meta-Xylene	3.26	10	0.52	0.11		
	(7.1)		20	0.87	1.04	5.92	147
			30	1.48	1.70		
			60	2.75	2.71		

TABLE 5

Calculated Intercepts (A), Correlation Coefficients (CC), and Relative Mean Deviations (RD)

Zeolite	Adsorbate	A	CC	RD (%)
H-ZSM-11	*para*-Xylene	0.584	0.95	10.7
	meta-Xylene	0.336	0.96	8.5
	ortho-Xylene	0.065	0.98	8.9
H-ZSM-5 (II)	*para*-Xylene	0.372	0.93	15.1
	meta-Xylene	−0.149	0.97	10.7
H-ZSM-5 (I)	*para*-Xylene	−0.444	>0.99	7.3
	meta-Xylene	−0.316	0.99	14.0

Catalytic Activity for Xylene Isomerization

Data for the ZSM zeolites are listed in Table 6.

In Fig. 4, one can observe the straight lines of $-\ln[(Q_\infty - Q_t)/Q_\infty]$ vs t, relative to *para*-xylene adsorption on the three zeolites; the best fit of experimental values with interpolated lines is obtained with the ZSM-5 (I). The following sequence in time-ratios (Table 4 and Fig. 4) is reported:

$$\text{HZSM-5 (I)} > \text{HZSM-5 (II)} \simeq \text{HZSM-11}$$

With respect to the ZSM-11 zeolite, the xylene isomer diffusivities follow the sequence: *para* ≫ *meta* > *ortho*, which corresponds exactly to the reverse of the critical molecular diameters: *para* < *meta* < *ortho*. The same results are observed for the ZSM-5 zeolites. Surprisingly, a different sequence is found for the sorption capacities at equilibrium, i.e., *para* > *ortho* > *meta* (Table 4).

TABLE 6

meta-Xylene Isomerization Activities[a]

Catalyst	TEQA[b]	SC8 (%)	P/O	P/m
H-ZSM-11	94.9	97.9	1.1	1.1
H-ZSM-5 (II)	97.9	99.5	1.2	1.1
H-ZSM-5 (I)	38.5	99.5	3.3	1.6
Amorphous[c]	1.6	100.0	1.3	1.1

[a] Reaction conditions: feed = pure *meta*-xylene; temperature = 325°C; pressure = 16 ata (1.62×10^6 N/m^2); molar H_2/*meta*-xylene = 5; liquid hourly space velocity = 6.

[b] TEQA = $\dfrac{100 - (\%\ meta\text{-xylene})(\text{out})}{100 - (\%\ meta\text{-xylene})(\text{thermodynamic equilibrium}} \times 100(\%)$.

[c] Silica-alumina from a ZSM-5 preparation with zero crystallinity (reaction conditions = the same as in *a*).

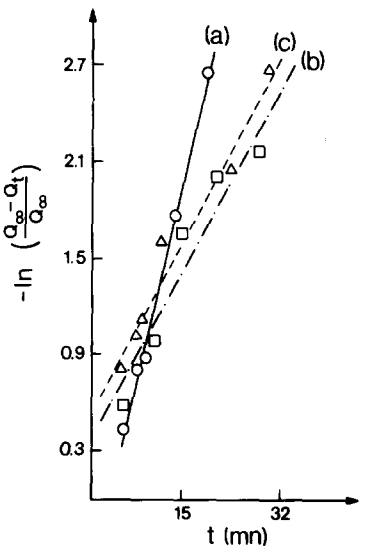

FIG. 4. *para*-Xylene sorption: experimental values and interpolated straight lines of $-\ln[(Q_\infty - Q_t)/Q_\infty]$ vs t. (a) H-ZSM-5 (I), ——○——; (b) H-ZSM-5 (II), --□--; (c) H-ZSM-11, --△--.

The analogy in physical (degree of crystallinity, mean diameter of particles, and their size distribution), chemical (Si/Al atom ratio), and sorptive properties (nitrogen, *n*-hexane, and water sorption capacities, RAI and xylene isomer diffusion factors) (Tables 2 and 4) seems to agree with the similarity in catalytic performance in the *meta*-xylene isomerization (Table 6). Nevertheless, the slight difference in structure between these two zeolites (*5*, *6*) both belonging to the Pentasil family (*15*) has not led to any difference in diffusive and catalytic data.

The differences occurring between the two ZSM-5 samples are the mean diameter and size distribution of the crystalline particles, and intracrystalline sorption data. Therefore, it is useful to have a correlation with their differences in catalytic activity.

As shown in Table 6, the ZSM-5 (II) is more active but less selective (with respect to the *para*-xylene) than the ZSM-5 (I). The greater activity of the ZSM-5 (II) should be explained at first by a higher sorption capacities with all the tested molecules which undergo an intracrystalline sorption (see Tables 2 and 4) and in particular with the *meta*-xylene which is the reacting molecule. A cooperative effect might come from a suitable stronger acidity of the active sites, since the *meta*-xylene isomerization is an acid-catalyzed reaction (*16*). In fact, even if the two ZSM-5 samples involved, both in the H-form, have the same sodium content (see Table 2), the as-made form of the ZSM-5 (II) has a Na percentage nearly three times higher than that of the ZSM-5 (I) (see Table 3). Since sodium level differences between the Na and the H-forms may reflect the acid strength of the active sites within the zeolite pore, an explanation based on the previous observation may be given in connection with the zeolite activity in the acid-catalyzed isomerization. However, further studies in acid strength and density, and in the acidity-generating exchange effects are needed.

On the contrary, the higher *para*-xylene selectivity of the ZSM-5 (I) may be ascribed to the ability for the *para*-xylene, as reaction product, to diffuse rapidly to the boundaries of the crystalline particles of the zeolite. In fact, the comparison of the diffusivities and of *para*-xylene to *ortho*- and *meta*-xylene selectivity ratios between the two ZSM-5 samples (see Tables 4 and 6) gives the following result:

H-ZSM-5 (I): (D_{para}/D_{meta}) = 4.3; P/O = 3.3; P/m = 1.6

H-ZSM-5 (II): (D_{para}/D_{meta}) = 1.8; P/O = 1.2; P/m = 1.1

As to the H-ZSM-11, we have:

(D_{para}/D_{meta}) = 2.1; P/O = 1.1; P/m = 1.1

Such high selectivity for *para*-substituted alkyl-aromatics is frequently observed in the literature when a zeolite structure like ZSM-5 having relatively large crystals is used as adsorbent or catalyst, e.g., Ref. (*17*).

We have shown that sorption and diffusion data can correlate the physical characteristics of isostructural or structurally different zeolites with their catalytic properties. However, the absolute values of the diffusion coefficients D still constitute the factors of uncertainty because of the ambiguity in the definition of the radius a. A choice is frequently made on the mean crystallite radius (*18*). Since the use of Eq. (1), valid only for large sorption times, implies a precise knowledge of the crystallite shape and size distribution, which may strongly affect the diffusion coefficient calculation (*19*), the obtaining of reasonably reproducible and comparable values for parameter a needs the production of large and well-formed zeolite crystallites and the employment of sophisticated techniques such as SEM. For workers in the applied catalysis field, this may imply a really great "Chinese puzzle" because large and homogeneously distributed crystallites, readily measurable as in the case of an A-type zeolite (*20*), are extremely difficult to obtain with the present state of the ZSM synthesis art and/or do not always correspond to a sufficiently high catalytic activity needed to justify onerous research efforts for their production.

CONCLUSIONS

Although there are some theoretical and practical limitations, the proposed method for diffusion study is faster and simpler in experimental measurement and data elaboration than other static or dynamic techniques. Nevertheless, Barrer's formula (valid in this case for large sorption times) may be very advantageous for researches in applied catalysis; in fact, since the present method can cover a range of relative sorption from 10 to 100%, it seems to be suitable for studies of the overall diffusion phenom-

ena which involve the maximum of the active sites as encountered in an optimized catalytic reaction. However, modification of the apparatus is foreseen for the measurement of vapor diffusion in presence of a carrier gas and in static conditions of sorption. In this case, a comparison with previously obtained diffusion coefficients might be made (*21*).

Our data emphasize the high selectivity of the ZSM zeolites to *para*-xylene. They also show that xylene diffusion in the ZSM is strongly affected by the molecular conformation of the diffusant. When the physicochemical characteristics and the consequent sorptive properties are very similar between a ZSM-11 and a ZSM-5 zeolite, no difference in xylene diffusion and catalytic data is observed.

On the other hand, it is shown that the ZSM shape selectivity in *meta*-xylene isomerization may be mainly related to the diffusivity of the product molecules (by comparison with the reactant or other reaction products), while their activity may be principally influenced by their sorptive capacity with respect to the reactant and by the acidity characteristics of their active sites. The comparison of sorption and diffusion data between two ZSM-5 samples which have the same chemical composition and the same degree of crystallinity has led at first to the conclusion that the diversity in selectivity to *para*-xylene in the *meta*-xylene isomerization reaction depends strongly on their crystalline particle dimension and size distribution. These size characteristics are determined by a thin silica binding deposit between the small microcrystals, the effect of which is a slight restriction in intracrystalline accessibility to all molecules and a higher selectivity to *para*-xylene. Further studies are needed to elucidate the actual nature of this silica cement within the large aggregates but we believe already that its "screening" action on bulky molecules such as xylenes is similar to that of the "postsynthesis" modification involving depositing silica (*22*) or phosphorus [(*23*), and references therein] onto the ZSM zeolites.

Therefore, by choosing precise synthesis parameters, we have obtained an analogous "enhanced" selectivity towards the *para*-dialkylaromatic product as observed in the studies cited (*22, 23*).

APPENDIX

The influence of intercrystalline diffusion has also been verified by applying the method proposed by Kočiřik and Zikánová [(*24*) and Ref. (*3*), p. 279]. According to this method intraparticle diffusion is rate controlling if:

$$E_2 = E_1 - \frac{a^2}{15pD_g} \gg \frac{a^2}{15pD_g} \qquad (2)$$

where p is the fraction of the adsorbate molecules in the intercrystalline space (about the external porosity of the bed of pseudo-spherical particles), D_g the diffusion coefficient in the interparticle space, E_1 the first statistical moment (*3*), and E_2 the contribution to E_1 of intraparticle (or intracrystalline) diffusion.

At the pressures and temperature indicated in Table 1 the mean free path of xylene molecules is about 1.5 μm; this value is much smaller than the interparticle distance for particles with diameter 10–30 μm (Table 2). Therefore we can calculate D_g with the equation for free self-diffusion (*25*); it results that $D_g \simeq 2$ cm^2/sec. Assuming $0.26 < p < 0.34$, due to the diameter of the pseudo-spherical particles, one derives a value of $a^2/(15pD_g)$ ranging from 2×10^{-8} to 2×10^{-7} sec. For the seven runs reported in Table 4 the value of E_1 (sec) is, respectively: 590;1300;2650;775;1800;570;2400. Therefore it is well verified that $E_2 \gg a^2/(15pD_g)$ and that intraparticle diffusion is rate controlling.

ACKNOWLEDGMENTS

The authors thank Dr. V. Zamboni for helpful discussions, and Drs. A. Marzi, E. Moretti, M. Padovan, and M. Solari for technical assistance.

REFERENCES

1. Le Van Mao, R., *React. Kinet. Catal. Lett.* **12,** 69 (1979).
2. Le Van Mao, R., Pilati, O., Marzi, A., Leofanti, G., Villa, A., and Ragaini, V., *React. Kinet. Catal. Lett.* **15,** 293 (1980).
3. Barrer, R. M., "Zeolites and Clay Minerals as Sorbents and Molecular Sieves," p. 273. Academic Press, New York, 1978.
4. Crank, J., "The Mathematics of Diffusion," 2nd ed., p. 91. Clarendon Press, Oxford, 1975.
5. Argauer, R. J., and Landolt, G. R., U.S. Pat. 3702886 (1972).
6. Pochen, Chu, U.S. Pat. 3709979 (1973).
7. Lippens, B. C., and De Boer, J. H., *J. Catal.* **4,** 319 (1965).
8. Gregg, S. J., and Sing, K. S. W., "Adsorption, Surface Area and Porosity," 2nd ed., p. 214. Academic Press, New York, 1982.
9. ASTM-Committee D-32 on Catalysts, "Standard Method for Determining Zeolite Area of a Catalyst," Philadelphia, 1982.
10. Sing, K. S. W., *Chem. Ind.* 829 (1967); 1520 (1968).
11. Mieville, R. L., *J. Colloid Interface Sci.* **41,** 371 (1972).
12. Johnson, M. F. L., *J. Catal.* **52,** 425 (1978).
13. Breck, D. W., "Zeolite Molecular Sieves," Wiley, New York, 1974.
14. Derouane, E. G., Detremmerie, S., Gabelica, Z., and Blom, N., *Appl. Catal.* **1,** 201 (1981).
15. Kokotailo, G. T., and Meier, W. M., "The Properties and Application of Zeolites," p. 133. Townsend, London, 1979.
16. Poutsma, M. L., *ACS Monograph* **171,** 437 (1976).
17. Chen, N. Y., Kaeding, W. W., and Dwyer, F. G., *J. Amer. Chem. Soc.* **101,** 6783 (1979).
18. Eberly, P. E., *ACS Monograph* **171,** 392 (1976).
19. Ruthven, D. M., and Loughlin, K. F., *Chem. Eng. Sci.* **26,** 577 (1971).
20. Yucel, H., and Ruthven, D. M., *JCS Faraday I* **76,** 60 (1980).
21. (*a*) Ragaini, V., Mazzola, E., and Bart, J. C. J., *Z. Phys. Chem. N.F.* **115,** 43 (1979); (*b*) Ragaini, V., Giupponi, M., and Bart, J. C. J., *Z. Phys. Chem. N.F.* **119,** 85 (1980).
22. Rodewald, P. G., U.S. Pat. 4090981 (1978).
23. Védrine, J. C., Auroux, A., Dejaifve, P., Ducarme, V., Hoser, H., and Zhou, S., *J. Catal.* **73,** 147 (1982).
24. Kočiřik, M., and Zikánová, A., *Ind. Eng. Chem. Fund.* **13,** 347 (1974).
25. Reid, R. C., Prausnitz, J. M., and Sherwood, T. K., "The Properties of Gases and Liquids," p. 551. McGraw-Hill, New York, 1977.